p. 52

P-26

CRITICAL POINT WETTING DROP TOWER EXPERIMENT

FINAL REPORT

for NAG8-511

April 18, 1990

by

William F. Kaukler

Department of Chemistry, The University of Alabama in Huntsville, Huntsville, Alabama 35899

Abstract

This report summarizes the experimental results from NASA Headquarters Grant NAS8-511. The 100 m Drop Tower at Marshall Space flight Center was used to provide the step change in acceleration from 1.0 g to 0.0005 g. An inter-fluid meniscus oscillates vertically within a cylindrical container when suddenly released from earth's gravity and taken into a microgravity environment. Oscillations damp out from energy dissipative mechanisms such as viscosity and interfacial friction. Damping of the oscillations by the later mechanism is affected by the nature of the interfacial junction between the fluid-fluid interface and the container wall.

In the earlier stages of the project, the meniscus shape which developed during microgravity conditions was applied to evaluations of wetting phenomena near the critical temeperature. Variations in equilibrium contact angle against the container wall were expected to occur under critcal weting conditions. However, it became apparent that the meaningful phenomenon was the damping of interfacial oscillations. This latter concept makes up the bulk of this report.

Perfluoromethylcyclohexane and isopropanol in glass were the materials used for the experiment. The wetting condition of the fluids against the wall changes at the critical wetting transition temperature. This change in wetting causes a change in the damping characteristics of the interfacial excursions during oscillation and no measurable change in contact angle. The effect of contact line friction measured above and below the wetting transition temperature was to increase the period of vertical oscillation for the vapor-liquid interface when below the wetting transition temperature.

UAH Thrust Area: Microgravity Materials Science

Discipline: Chemistry and Physics of Fluid Interfaces

Key Words: Drop Tower, Interfaces, Wetting, Microgravity, Critical Temperature, Immiscible Fluids

TABLE OF CONTENTS

Introduction and Objectives

Observations of inter-fluid menisci formed in an axisymmetric container during a step reduction in acceleration were made. Evidence of a wetting transition was sought by analyzing meniscus characteristics. Fluid wetting, pressure and container geometry determine meniscus shape. A reduction of gravity reduces the pressure in the fluids. This was done by using the Marshall Space Flight Center (MSFC) Drop Tower facility. By unloading the hydrostatic pressure in this controlled way, interface oscillations are started and interfacial forces are no longer masked by earth gravity. Damping of the oscillations occurs during the period of microgravity as a result of viscosity and of the dissipation of energy at the contact line where the menisci meet the container. This will be discussed later. Microgravity conditions extending up to three seconds (of the 4.5 second drop) are obtained in the Drop Tower. (High quality low-g conditions were always available for the first 2.4 seconds.)

During the project, the approach and objectives shifted and evolved into those summarized in Table 1. The rationale for these changes will be made clear.

Critical Wetting Theory

In 1977, Cahn[1] introduced the Critical Point Wetting (CPW) theory. Verification of the CPW theory is the main purpose of the experiments. Cahn predicted an abrupt transition from partial wetting to complete wetting could occur between two fluid phases against a third, inert phase during heating to the consolute temperature. Detailed development of the theory are found in the listed references[1,3,12,13]. A brief description is given here.

Between a wetting temperature (T_W) below the consolute (or critical) temperature (T_C) and the T_C of a two-fluid system, one fluid phase is expected to preferentially wet another inert phase (eg. container or vapor phase). The non-wetting phase will lose contact with the inert phase completely. Cahn showed CPW has universal applicability to any immiscible system.

To describe fluid wetting a solid surface, Young's equation may be used. You may refer to Figure 1. In this equation, the interfacial free energies, σ, of the two fluids, 1 and 2, and the solid surface S, are related through a contact (or wetting) angle θ.

$$\sigma_{1,2}\cos\theta = \sigma_{1,s} - \sigma_{2,s} \qquad (1)$$

A result of the full wetting condition when above T_W, from the solution of Young's equation[1], is the zero contact angle formed by the inter-fluid interface and the non-critical surface (glass). Below the T_W, partial wetting and thus, non-zero contact angles are expected.

This phenomenon is difficult to observe in earth gravity due to the *sedimentation effect* which causes the more dense phase to lay under the less dense phase, often with an essentially flat meniscus. Contact angle evidence of the wetting transition is obscured by gravity. Other factors such as T_W existing below the melting point, and some T_W's being very close to T_C have made the experimental observation of this wetting phenomenon an elusive one.

Previuous Experimental Evidence of CPW

Although CPW theory was recently discovered, a number of phenomena have been attributed to it. Table 2 summarizes various applications of the theory.

There have been some previous observations of CPW. The initial observations of vanishing contact angles below the critical temperature by Heady and Cahn[2] lead to the CPW theory. Moldover and Cahn then showed how the wetting transition could be manifest with small changes in the water content of cyclohexane-methanol mixtures[3].

Zabel et al found CPW caused a thin film of one hydrogen rich phase (α) to surround another hydrogen rich phase (α') in crystals of niobium[5].

Grugel and Hellawell used CPW theory to explain monotectic microstructure development based on the comparison between the temperatures for the critical and freezing points[4]. Interpreted diagrams based on Hellawell's empirical theory of how monotectic microstructure is affected are shown in Figure 2 (a) and (b). Figure 2(a) shows a view of a *regular monotectic* freezing front. Figure 2(b) shows a high and low dome monotectic phase diagram Table 3 shows some monotectic systems and their structures.[4] The value of 0.9 for the T_M/T_C (T_M = the monotectc temperature) was found to be the breakover point. Below 0.9, a regular or aligned monotectic microtructure results while above the breakover point, an irregular structure is formed. Irregularity is caused by the low dome condition resulting in a depression of the wetting temperature to a point below the freezing or monotectic temperature. Solidification must proceede under critical wetting conditions and irregularity is the effect.

Contact Line Phenomena

Spreading of fluids on solid surfaces has recently been studied more closely[6-11]. Experimentally, one encounters the phenomenon of contact angle hysteresis (CAH). Here a contact angle is reproducibly measured after the spreading of fluid over a solid surface, and subsequently a different, usually smaller contact angle is measured after the fluid recedes[7]. It is possible the fluid will not move over the surface until these extremes of contact angle are exceeded. These conditions apply to a static (equilibrium) contact angle measurements. CAH has been attributed to surface roughness or other irregularities on the surface since it can be minimized by polishing the surface.

The consideration now is directed to dynamic contact angles, those established during the movement of the fluid interface. Experiments have shown there is a contact angle dependence on contact line velocity[6, 8, 9, 11], see Figure 3. The static CAH limits are the two values of θ where U = zero, that is, the intersection of the CA vs. U lines (for each substrate) with the CA axis for zero contact line velocity. More significantly, there is a variation in θ with velocity. Young and Davis[9] found that both the CAH and steepening of the contact angle with increasing contact line velocity are dissipative effects. For example, wave amplitude against a vertical wall (gravity waves) is dampened not only by viscosity but also by the contact line *friction* against the wall.

If a wetting layer of lower phase is formed between the upper phase and the container and/or vapor (at temperatures above T_W), then the contact line *friction* should be different from that for partially wetting conditions found at temperatures below T_W. This layer of the lower phase separates the upper phase from the glass and vapor. The contact line which sweeps up and down is no longer the tri-junction between the upper fluid, lower fluid and the glass phases.

It is known that fully wetting fluids do not have contact angle hysteresis (as the contact angle is zero). We cannot expect the magnitude of the dissipative effects at the contact line to be the same during partial wetting conditions. Young and Davis[9] state that the dissipative effect of contact angle steepening with increased contact line speed is suppressed for cases of fixed contact angle and fixed contact line when the contact line is independent of contact line speed. Full wetting means fixed contact angle. Increased dissipation of the meniscus oscillation is therefore expected for $T < T_W$.

Differentiating the dissipative effect of viscosity from that of contact line *friction* is possible when experiments are performed with conditions such that the rate of relaxation of the fluid at the solid-liquid-gas junction is much greater than the velocity.[11] Johnson et al could ignore viscosity effects for their experiments[11] because their conditions satisfied the above assumption.

Experiment Technique

The experiments described here rely on the gravity environment produced by the Drop Tower. Initially, the experiment package (270 kg and 1x1x1 meter dimensions) sits within the drag shield shown in Figure 4 at the top of the tower (100 meters nominal). Upon release, a pressurized gas rocket thruster accelerates the (over 1000 kg) drag shield with 45 to 50 pounds of thrust such that the experiment package floats up from the drag shield floor (about 5 cm). Microgravity conditions within the experiment begin at this point and have levels reaching 10^{-3} to 10^{-5} g. The drag shield ensures air drag doesn't influence the experiment. The thrusters keep the drag shield falling with the rate of 1 g.

The drag shield is decelerated by a catch tube (see Figure 4) which permits a controlled release of compressed air as the close fitting drag shield enters the tube. The package settles on the floor and finally all comes to rest with up to a maximum of 31 g deceleration.

The experiment package houses several subsystems: a) circulating oil bath with windows and the specimen(s), b) temperature controller for the bath, c) high speed (500 fps) 16mm movie camera, d) 3-axis accelerometers and data acquisition electronics, e) NASA low-g accelerometers and telemetry, f) timing and switching circuits g) batteries and h) lights for photography. Figure 4(b) shows a schematic of this package configuration. The camera views through the window of the bath at the specimen. The specimen is illuminated from behind by a light bank and diffuser. The camera is allowed to get up to speed prior to release. An LED display of time in hundredths of a second is filmed simultaneously with the specimen. Other LED's mark the moment of release and of the package contact with the drag shield floor. Accelerometer data is time marked to permit synchronizing all data later.

The experiment package setup and hardware evolved to the above description after a couple of years of testing. Further evolution followed where the NASA accelerometers were replaced by Sundstrand 1200 accelerometers and telemetry of the acceleration dispensed with. The 16mm movie camera was replaced with a high resolution EDO Western black and white high resolution Newvicon tube video camera. Video images were transmitted by an IR laser video telemetry system from LACE Comunications. A shematic of the video hookup at the Drop Tower Facility is shown in Figure 5. Video was used to monitor the experiment before and after the drop for saftey, pre-drop checkout and data collection. The optics were improved to increase the magnification to the point that the two meniscii in the ampoule filled the field of view. This was not possible with the 16mm Milliken cameras. A fixed frame rate of 30 frames per second is obtained with the video. Viewing half of an interlaced frame would give 60 frames per second.

Changes in the wetting behavior of the two immiscible fluids and their vapor were studied in this experiment by varying the temperature of the system about the wetting transition temperature. Specimens consist of glass cylindrical ampoules (with 2.5 cm ID) partially filled with perfluoromethylcyclohexane (C_7F_{14}) and isopropanol ($i\text{-}C_3H_7OH$) (here called PI) fluid phases. See Experimental Analysis for details on the PI system. A photograph of the specimen showing the menisci formed in unity gravity is shown in Figure 6(a). Figure 6(b) shows the specimen at steady state after 2.3 seconds of micro-g. There are two menisci in each specimen, the upper one (concave up) between the vapor and upper liquid phase, the lower one (concave down) between the two immiscible liquid phases. Meniscus geometry as well as how the interfaces respond to the microgravity induced oscillations is photographically recorded during the experiment. Drops are made at various temperatures about T_W and below T_C to determine the interfacial energy variation as a function of temperature.

Prior to the drop, the specimen is closely held at temperature as long as one day within the silicone-oil bath. Interfacial tension relationships between the phases will otherwise change with temperature[1,7,12,14]. The most important information to obtain experimentally is acceleration level, temperature and interface behavior. All the package subsystems are mounted to the same frame structure. The specimen sits near the package center of gravity and the package itself is balanced so that a clean release from the drag shield floor occurs at the onset of acceleration.

An experiment runs for only eight seconds total time. A drop takes a day to prepare. Full free-fall of the experiment lasts 3.5 seconds. Oscillations of the fluid interfaces can have frequencies of less than two Hertz up to ten Hertz. As a result, high motion picture frame rates or video is used to dissect the time domain of the fluid motions. (Errors in measuring the interface shape and position are statistically reduced by using the many frames available.)

Why Use a Drop Tower for Wetting Experiments?

Surface tension (interfacial free energy) causes the menisci profiles to decrease in radius in lower-g according to the Bond number B_0,

$$B_0 = \frac{\delta g (d^2/2)^2}{\sigma} \qquad (2)$$

where δ is the density difference between the upper and lower fluid phase, d is the ampoule diameter, and is the interfacial free energy or surface tension. A B_0 of zero calls for a perfectly spherical meniscus profile. While the Bond number controls the shape of the meniscus between the walls of the container, the contact angle determines the angle the interface makes against the wall. Shape differences that the Bond number change creates are shown in Figure 7.

Smaller radii of interface curvature are easier to measure experimentally. This is one reason why many fluids experiments have been done in the Space Shuttle in micro-g. Each of the four variables in the B_0 expression can be adjusted to gain maximum sensitivity. The size scale of the ampoule can reasonably be adjusted only by an order of magnitude (millimeters to centimeters). Smaller capillary lengths would render CPW and other fluid effects unobservable while larger ampoules would be impracticable to wield. Density differences and interfacial free energy can be adjusted to vary over a small range by changing temperature. These are relatively narrow adjustment ranges.

Using the Drop Tower facility, the acceleration level can be adjusted from unity down to as low as 10^{-5} g. This represents a five order of magnitude range, and done without compromising any other variables. Figure 8 shows comparative Bond number differences for a few organic immiscible systems under similar circumstances of 1 cm diameter containers and unity gravity.

Fluid motion responses to changes in acceleration are generally brief when the capillary length is as short as it is in these specimen ampoules. Curvature change in the menisci is not instantaneous upon going from unity g to micro-g. Each of the two menisci in the ampoule oscillate at their own rates for a cycle or two before coming to the equilibrium shape predicted from the respective B_0's.

Since the change in g-level is a near perfect step (from 1 g to 10^{-4} g), the system is not prone to secondary, artifact producing effects, such as vibration, mechanical friction etc. Small lateral forces ($< 10^{-4}$ g) are generated, but this problem is presently being minimized. Every drop in the Drop Tower produces reproducible conditions which would be very difficult to recreate in the laboratory by some other mechanism. Extended periods of micro-g are not really needed, and the experiment need not be qualified for flight. When multiple experiments are required, improvements can be easily introduced between tests. This makes the Drop tower an ideal research tool for this type of work.

Experimental Analysis

The PI (C_7F_{14} and i-C_3H_7OH) system used by Schmidt and Moldover[12,13] is the one best documented immiscible system with a measured CPW transition. The critical temperature, T_c, is 90.5 ±0.5°C, and the T_W was found to be 38.0 ±0.1°C. These temperatures are marked on the phase diagram, Figure 9. At temperatures above T_w, the more dense C_7F_{14}-rich phase (with density of 1.768 g/cm at 22°C) will form a wetting layer between the vapor phase and the upper, less dense C_3H_7OH-rich phase (of density 0.826 g/cm at 22°C). Experiments were performed in the temperature range 35 to 55 °C, encompassing the T_w.

Full thermodynamic equilibrium is assumed. Experimentally, the prerequisite for this is a constant temperature and no agitation that could disturb the compositions of the fluids near the interphase interfaces. A static contact angle can form in about 2 seconds after release in the drop tower, but true equilibrium compositions in the vicinity of the interfaces cannot be reached in the seconds available.

All Drop Tower drops performed on this project have been tallied in Table 4. As can be found from this table, many of the drops did not yield solid data. The experiments have been inflicted with difficulties from many sources. While funding was for one year, this funding was stretched out for over four years due to the many delays in performing the drops. There is some data obtained near the end of the grantthat has yet to be analysed.

A Fortran computer code for meniscus shapes in both rectangular and cylindrical cuvettes has been acquired from Roberts and Associates. The programs are made to operate on an IBM-PC type machine and draw meniscus shapes on an EPSON printer.
Calculated points are saved in a file as well and better plotting methods can be used to view the calculations. This code was also implemented in analysis of KC-135 experiments performed in square cross section cuvettes of succinonitrile and ethanol solutions. The interface shape changes at various temperatures were photographed and the work was done in conjunction with the drop tower experiments. Results of these are not presented here.

Results and Observations

At first, the contact angle between the interfluid phases and the container wall as well as the overall meniscus shape were the most important sources of proof that a wetting transition had occured[14]. Due to the presence of small lateral g-forces during a drop and very low interfacial energy, the $liquid_1$-$liquid_2$ meniscus became distorted. The meniscus shape (contact angle and curvature) determinations were not sufficiently precise due to the residual lateral accelerations caused by the weak restraints that data cables placed on the experiment pallet. Interfacia_l oscillations did not damp out early enough to reach static equilibrium due to the limited low-g time available. The experiment would have worked except that for most of the drops when data were colectively good, the defective dragsheild rails would impart forces on the experiment prematurely. Instead of 3.5 seconds of low-g, for the most part, only 2-2.4 seconds were available. As a result, this approach was abandoned. However, the shape differences should still be a sensitive test for the critical wetting condition and better tower performance would have made this known.

An observation[15-18] was made of a subtle rate of oscillation period change when the temperature was raised from below T_w to above T_w. To show this, the excursion of the meniscus apex in the central vertical axis is plotted against time in Figure 10 and 11. Apex position was measured manually using a graphics tablet and a film projector. About a hundred points were taken from each sequence originally photographed at 500±4 frames per second. Specimen temperatures were 34.25 °C and 42.0 °C respectively for Figure 10 and 11. Both menisci within a specimen are plotted such that the upper and lower curves match the upper and lower menisci of Figure 6. Figure 6(a) shows conditions at time < zero in Figure 10 or 11, while Figure 6(b) shows conditions at time > 2.3 seconds until impact.

Displacement of the mid-section or apex of the fluid interface results in a symmetrically opposing movement of the contact line against the ampoule wall since there is no volume change. This is shown in Figure 12 using a calculated meniscus profile.

A dashed line marks the aproximate meniscus profile at one-g. The sides of the graph represent the ampoule walls. The inter-fluid interfaces *slide* up and down along the ampoule wall with certain velocities in response to the pulse change in g-level. The period of oscillation was found not to remain constant with each cycle. As the oscillations damped out, the velocity of the contact line on the ampoule wall also diminishes. Dissipation from the contact line *friction* is known to be a function of contact line velocity. In part, this stems from the variation in contact angle with velocity. This is discussed in the next section. As it is the wetting conditions at the wall which is being tested, altering the wetting conditions should affect the oscillation rate and damping of the oscillations.

Interfacial free energy, viscosity and density difference all diminish as temperature increases. There is no singularity in these functions. CPW is a first-order wetting transition which should manifest a singularity in Young's equation or in fluid layer thickness. By using the meniscus oscillations and comparing them in the temperature regime about T_W, the wetting transition should lead to a singularity in the damping behavior of these oscillations. There has been qualitative evidence to indicate there is an effect. More experiments would permit an empirical curve to be drawn showing the damping factor as a function of temperature. The wetting transition would then be clearly revealed.

The results shown here are the best that have been obtained to date. There are three results relating to the meniscus oscillation measurements:

There is clear evidence that the damping of the oscillation wave amplitude is greater for $T < T_W$ in the PI system. Careful comparison of Figures 10 and 11 will show the amplitude of the oscillations in the liquid-vapor interface are more strongly damped at 34.25 °C. This might be attributed to the increased viscosity. Viscosity, however is not the sole dissipation mechanism.

A difference in period of oscillation has been observed between temperatures above and below the T_W. Below T_W the frequency of oscillation for the vapor-liquid meniscus was measured to be 1.34 sec^{-1}, while above T_W the frequency was 1.25 sec^{-1}. This effect is due to the increase in interfacial free energy as temperature is decreased.

The observation that initiated the contact line *friction* concept is a very subtle difference in the rate the period changes as the meniscus oscillates during a drop between the temperatures above and below T_W. At $T < T_W$, the period of oscillation increases constantly. At $T > T_W$, the period remains constant. Note that this is a different effect than damping with constant fundamental frequency. Under the full wetting conditions, the contact line *friction* is reduced and a period change does not occur. CAH is not present under full wetting conditions.

To be meaningful, one must ensure viscous relaxation of the fluid is more rapid than the contact line velocity. Contact line velocity has been measured to have a maximum of 2.6 mm/sec for the vapor-liquid interface. This value places it roughly in the non-viscous controlled domain. To clearly show that contact line friction increases the period of oscillation during partial-wetting conditions, the data needs to be improved. Too few points taken from the meniscus vertex displacement with time result in noisy Fourier Transforms. (The subtlety of this measurement requires such spectral analysis techniques.)

Resolving the smaller, damped oscillations would also improve the data, but this would require more precision in the film registration within the movie camera and projector. To get around this problem, the video approach was being taken. Fewer frames per second were taken but automation of the image analysis is possible such that more frames can be measured per sequence. It is anticipated that more analysis from the collected results will be published in the future.

Conclusion

Critical Point Wetting may be demonstrated with the Drop Tower by observing interface behavior in the PI system. Differences in the measurements of the oscillation period and amplitude of the vapor-liquid menisci were shown between temperatures above and below T_W. Oscillation of menisci may be influenced by contact line *friction* which originates from the contact angle formed between the three phases that form the meniscus. An effect of this *friction* was the increased period of oscillation for the below T_W vapor-liquid meniscus.

Acknowledgment

This work has been funded by NASA Headquarters Grant NAS8-511. Thanks go to the support people for the MSFC Drop Tower; both to the UAH staff and to those from MSFC-NASA. Thanks are given to the Contract Monitor, Barbara Facemire at MSFC for her patience.

References

1. J. W. Cahn, "Critical Point Wetting", J. Chemical Physics, 66(8) (1977) 3667.

2. R. B. Heady and J. W. Cahn, J. Chem. Phys. 58 (1973) 896.

3. M. R. Moldover and J. W. Cahn, "An Interface Phase Transition: Complete to Partial Wetting", Science 207 (1980) 1073-1075.

4. R. N. Grugel and A. Hellawell, Met. Trans. A 12 (1981) 669.

5. H. Zabel, B. Schoenfeld and S.C. Moss, "Critical Point Wetting in NbH", J. Phys. Chem. Solids 42(10) (1981) 897-900.

6. E. B. Dussan V., "On the Spreading of Liquids on Solid Surfaces: Static and Dynamic Contact Lines", Ann. Rev. Fluid Mech. 11 (1979) 371-400.

7. P. G. de Gennes, "Wetting: Statics and Dynamics", Rev. Mod. Phys. 57(3) part I (1985)827-863.

8. E. B. Dussan V. and S. H. Davis, "Stability in systems with moving contact lines", J. Fluid Mech. 173 (1986) 115-130.

9. G. W. Young and S. H. Davis, paper submitted to J. of Fluid Mechanics, "A plate oscillating across a liquid interface: effects of contact angle hysteresis".

10. S. H. Davis, "Moving contact lines and rivulet instabilities. Part I, the static rivulet", J. Fluid Mech. 98 (1980) 225-240.

11. R. E. Johnson Jr., R. E. Dettre and D. A. Brandreth, " Dynamic Contact Angles and Contact Angle Hysteresis", J. Coll. and Int. Sci. 62(2) (1977) 205-212.

12. J. W. Schmidt and M. R. Moldover, "First-order wetting transition at a liquid-vapor interface", J. Chem. Phys., 79(1) (1983) 379-387.

13. J. W. Schmidt and M. R. Moldover, "The liquid-vapor interface of a binary liquid mixture near the consolute point", J. Chem. Phys., 83(4) (1985) 1829-1834.

14. W. F. Kaukler, "Critical Point Wetting Drop Tower Experiment", (Second Symposium on Space Industrialization, NASA Conference Publication 2313, Huntsville, Al. Feb. 1984).

15. W. F. Kaukler, "Critical Point Wetting Drop Tower Experiment" (Paper presented at 115th TMS Annual Meeting, New Orleans, La., 4 March 1986).

16. "Fluid Oscillation in the Drop Tower", Kaukler, W. F.; in Experimental Methods for Microgravity Materials Science Research, R. A. Schiffman Ed., The Minerals, Metals and Materials Society publisher, 1988, pp12-17.

17. "Fluid Oscillation in the Drop Tower", Kaukler, W. F.; Met. Trans. A, 19A Nov. 1988, pp 2625-2630

18. W. F. Kaukler, "Critical Point Wetting Drop Tower Experiment" (Paper presented at the Alabama Materials Research Conference, Huntsville, Al, Sept. 20, 1989).

TABLE ONE

C P W DROP TOWER EXPERIMENT
OBJECTIVES

- TEST CAHN'S CRITICAL POINT WETTING THEORY
- UTILIZE MICROGRAVITY TO UNMASK HYDROSTATIC FORCES
- LOOK AT A SUBTLE CHANGE IN THE WETTING CONDITION OF A FLUID AT A CONTAINER WALL BY OBSERVING OSCILLATORY BEHAVIOR
- APPLY INTERFACIAL 'FRICTION' ARGUMENTS TO EXPLAIN DAMPING OF FLUID OSCILLATIONS IN DROP TOWER
- TIE CRITICAL WETTING TO INTERFACIAL FRICTION

TABLE TWO

C P W DROP TOWER EXPERIMENT
APPLICATION OF THEORY

- CPW AFFECTS CONFIGURATION OF FLUID PHASES BELOW THE CRITICAL TEMPERATURE
- STRUCTURE OF MONOTECTIC COMPOSITES IS DEPENDENT ON CPW TEMPERATURE:
  - ALIGNED: HIGH CRIT T TO MONO T RATIO
  - IRREGULAR: LOW CRIT T TO MONO T RATIO
- NUCLEATION OF FLUID PHASES IS AFFECTED
- COMPOSITIONS OF LIQUID FILMS ARE AFFECTED

TABLE THREE

C P W DROP TOWER EXPERIMENT
MONOTECTIC REGULARITY

SYSTEM	Tm / Tc	STRUCTURE
SCN-WATER	0.88	ALIGNED
SCN-GLYCEROL	0.896	ALIGNED
SCN-BENZENE	0.91	IRREGULAR
SCN-ETHANOL	0.94	IRREGULAR
	‹0.9	ALIGNED
	›0.9	IRREGULAR

W. KAUKLER, UAH

TABLE FOUR

DROP TOWER DATA SUMMARY FOR CRITICAL POINT WETTING EXPERIMENT
FILM AND VIDEO DATA SET

DROP IDENT.	DROP DATE	TEMP C AT DROP	SYSTEM TESTED	DATA QUALITY	COMMENT
DT-12-84	5-10-84	?	SUCC/H2O	NONE	FAILURE
DT-1-85	3-29-85	?	SUCC/H2O	DARK FILM	FAILURE
DT-2-85	4-8-85	?	SUCC/H2O	NO FILM	FAILURE
DT-3-85	4-11-85	210	SUCC/H2O	DARK FILM	FAILURE
DT-4-85	4-12-85	209	SUCC/H2O		FAILURE
DT-5-85	?			NO FILM	FAILURE
DT-6-85	5-10-85	42.5	PF-ISO	NO FILM	FAILURE
DT-7-85	5-14-85	34.25	PF-ISO	GOOD FILM, NTI ACC.	GOOD
DT-8-85	5-14-85	42	PF-ISO	GOOD FILM, NTI ACC.	GOOD
DT-9-85	5-16-85	44.8	PF-ISO	NO FILM	
DT-10-85	10-4-85	?	PF-ISO	BAD DROP	
DT-1-86	8-6-86	35.1	PF-ISO	GOOD FILM, NTI ACC.	POOR LOW G
DT-2-86	8-21-86	55.8	PF-ISO	GOOD FILM, NTI ACC.	OK LOW G
DT-3-86	8-26-86	32.84	PF-ISO	NO TELEMETRY, GOOD FILM	
DT-4-86	8-26-86	34.03	PF-ISO	OUT OF FILM, NTI ACC.	OK LOW G
DT-5-86	8-28-86	76.18	PF-ISO	GOOD FILM, NTI ACC.	POOR LOW G
DT-1-87			PF-ISO		
DT-2-87			PF-ISO		
DT-3-87	4-16-87	11.75	PF-ISO		TEMP POST DROP
DT-4-87	5-4-87	47.9	PF-ISO	GEOTEK ACCEL.	
DT-5-87			PF-ISO	GEOTEK ACCEL.	NO DATA
DT-6-87	5-6-87	52	PF-ISO	NTI & GEOTEK ACCEL.	DENTED DRAG
SHEILD DT-7-87			PF-ISO	NTI & GEOTEK ACCEL.	OK LOW G
DT-1-88	2-10-88	56.6	PF-ISO	NTI ACCEL.	POOR LOW G
DT-2-88	2-23-88	47.25	PF-ISO	BAD NTI & GEOTEK ACC.	START USING VIDEO
DT-3-88	?		PF-ISO	GEOTEK ACCEL.	POOR VIDEO
DT-12-88	6-30-88	28.8	PF-ISO	GEOTEK ACCEL.	POOR VIDEO
DT-13-88	7-14-88		PF-ISO	GEOTEK ACCEL.	NO DATA
DT-14-88	7-26-88		PF-ISO	GEOTEK ACCEL.	NO DATA
DT-1-89			PF-ISO	GEOTEK ACCEL.	BAD VIDEO
DT-2-89			PF-ISO	GEOTEK ACCEL.	BAD VIDEO
DT-3-89			PF-ISO	GEOTEK ACCEL.	BAD VIDEO
DT-4-89			PF-ISO	GEOTEK ACCEL.	BAD VIDEO
DT-5-89			PF-ISO	GEOTEK ACCEL.	BAD VIDEO
DT-6-89			PF-ISO	GEOTEK ACCEL.	BAD VIDEO
DT-7-89	4-5-89	?	PF-ISO	GEOTEK ACCEL.	2.3 SEC LOW G
DT-8-89	4-20-89	50	PF-ISO	GEOTEK ACCEL.	LOST DATA
DT-9-89	4-27-89	50	PF-ISO	GEOTEK ACCEL.	LOST DATA
DT-10-89	5-2-89	40	PF-ISO	GEOTEK ACCEL.	NO VIDEO
DT-11-89	5-10-89	40	PF-ISO	GEOTEK ACCEL.	VIDEO OK
DT-12-89	5-17-89	42	PF-ISO	GEOTEK ACCEL.	VIDEO OK
DT-13-89	6-13-89	47	PF-ISO	GEOTEK ACCEL.	VIDEO OK
DT-14-89	6-20-89	43	PF-ISO	GEOTEK ACCEL.	VIDEO OK
DT-15-89	7-11-89	65	PF-ISO	GEOTEK ACCEL.	VIDEO OK
DT-16-89	7-13-89	23.8	PF-ISO	GEOTEK ACCEL.	AMBIENT TEMP.
DT-17-89	7-18-89	65	PF-ISO	GEOTEK ACCEL.	VIDEO OK
DT-18-89	7-20-89	65	PF-ISO	GEOTEK ACCEL.	ASSUME 65
DT-19-89	7-25-89	65	PF-ISO	GEOTEK ACCEL.	VIDEO OK

List of Figures

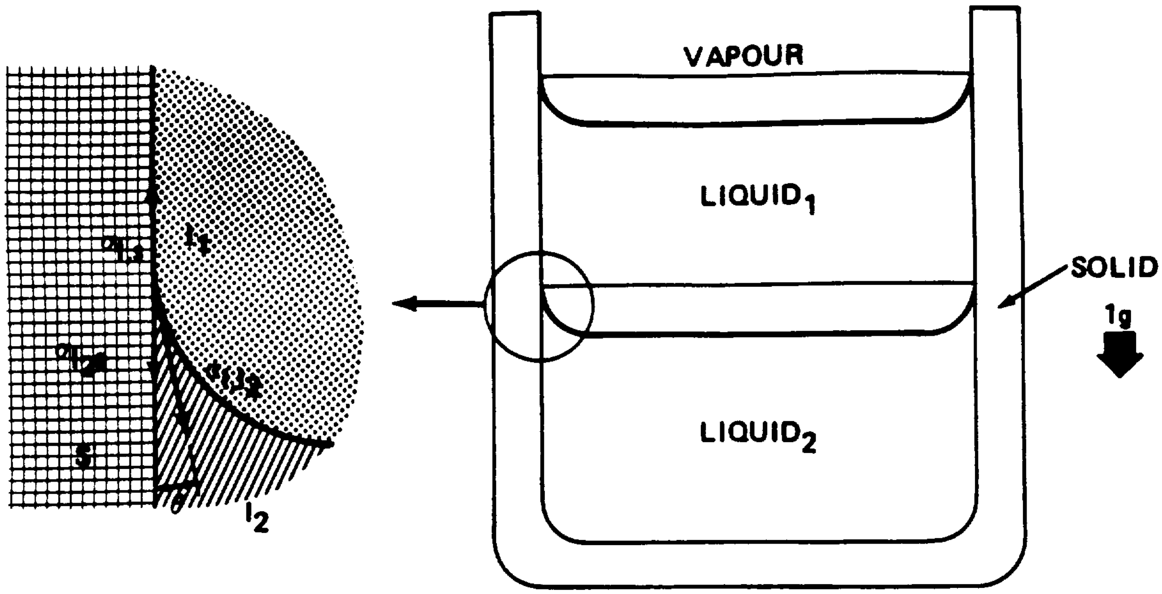

CONTACT ANGLE OF LIQUID IMMISCIBLES IN CONTAINER

FIGURE 1.

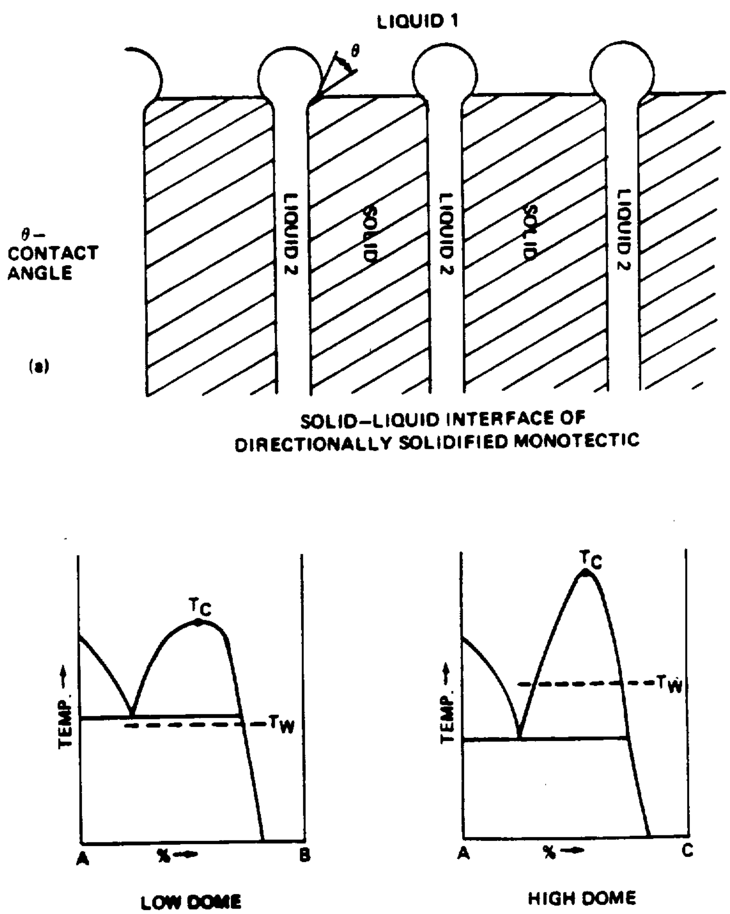

FIGURE 2. MONOTECTIC INTERFACE AND EXAMPLES OF HIGH AND LOW DOME MONOTECTICS

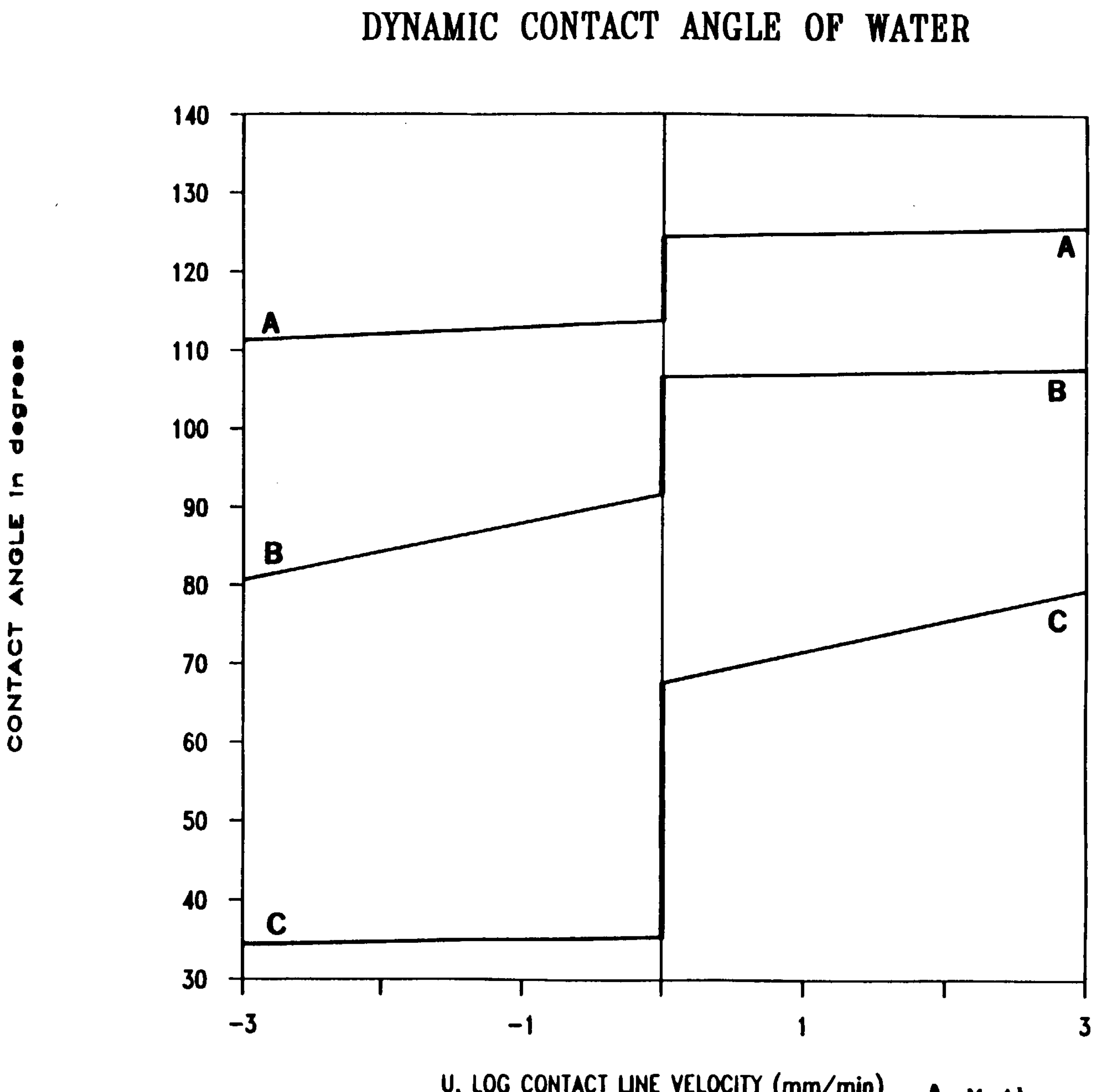

FIGURE 3.

A Methacrylate Fluoropolymer
B Siliconed Glass
C Trimethyl octacyclamonium chloride

DROP TOWER

DROP TOWER DETAILS

FIGURE 4.

SATURN V DYNAMIC TEST STAND DROP TOWER

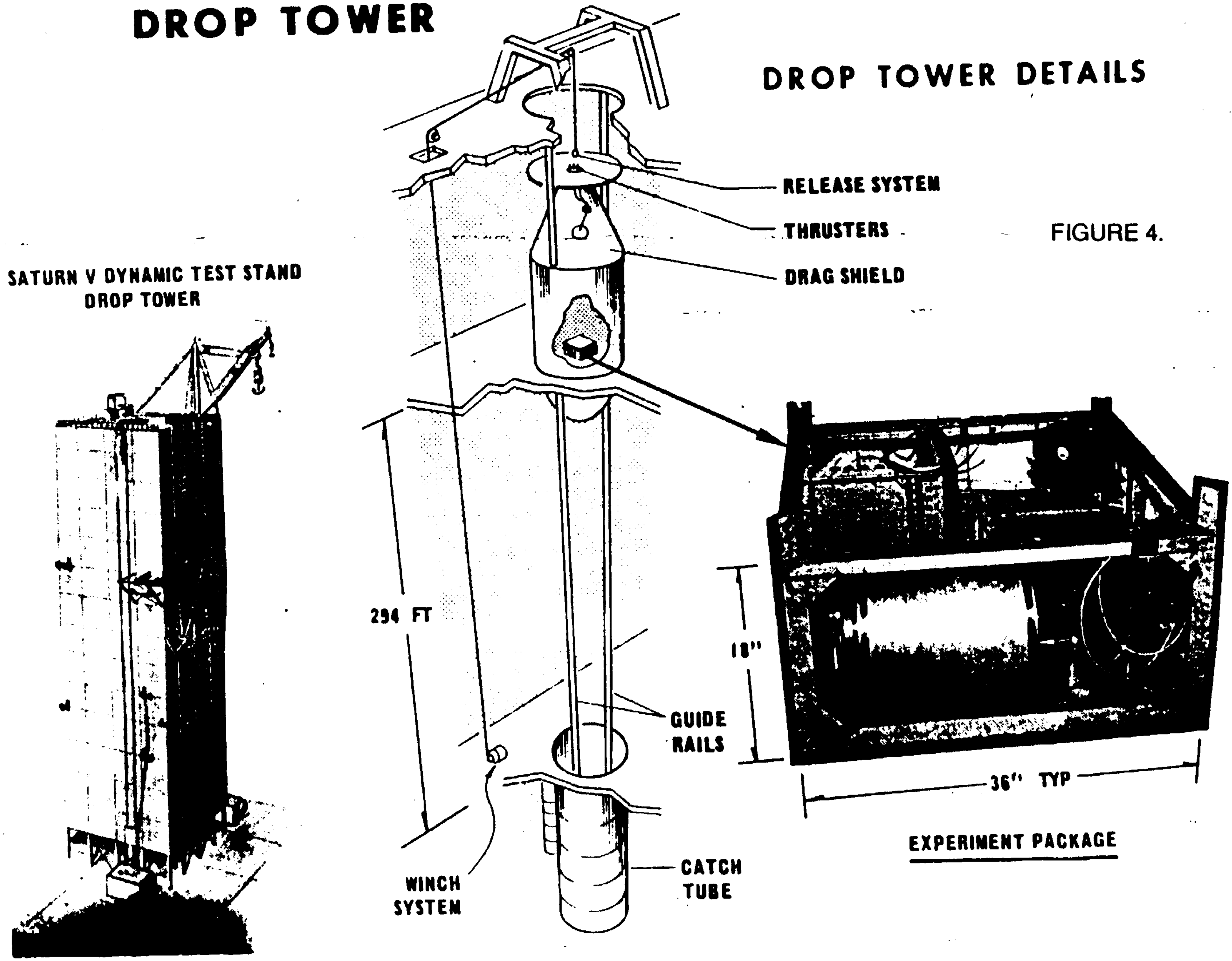

EXPERIMENT PACKAGE

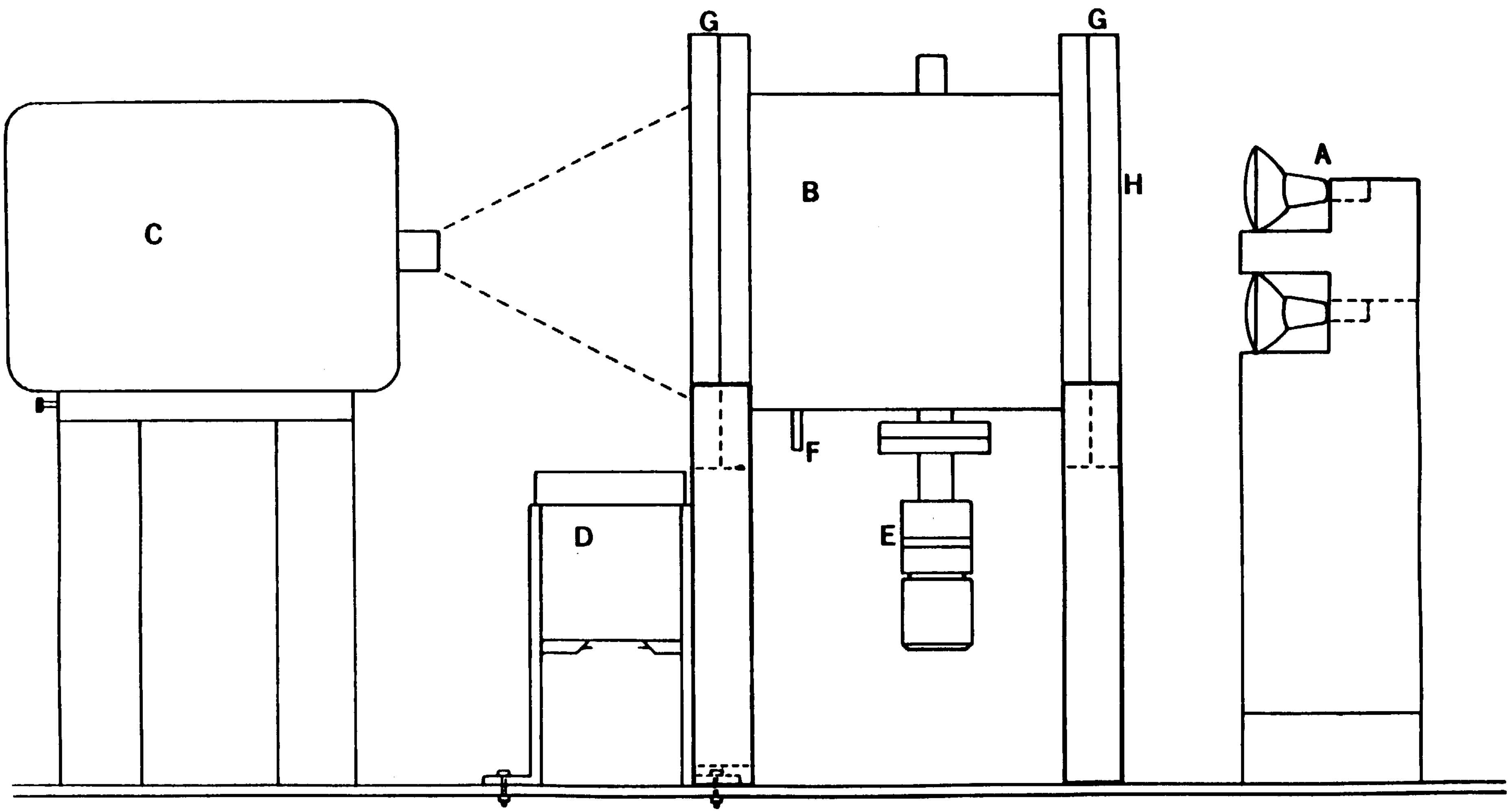

FIGURE 4(b).

VIDEO HOOKUP SCHEMATIC

FIGURE 5.

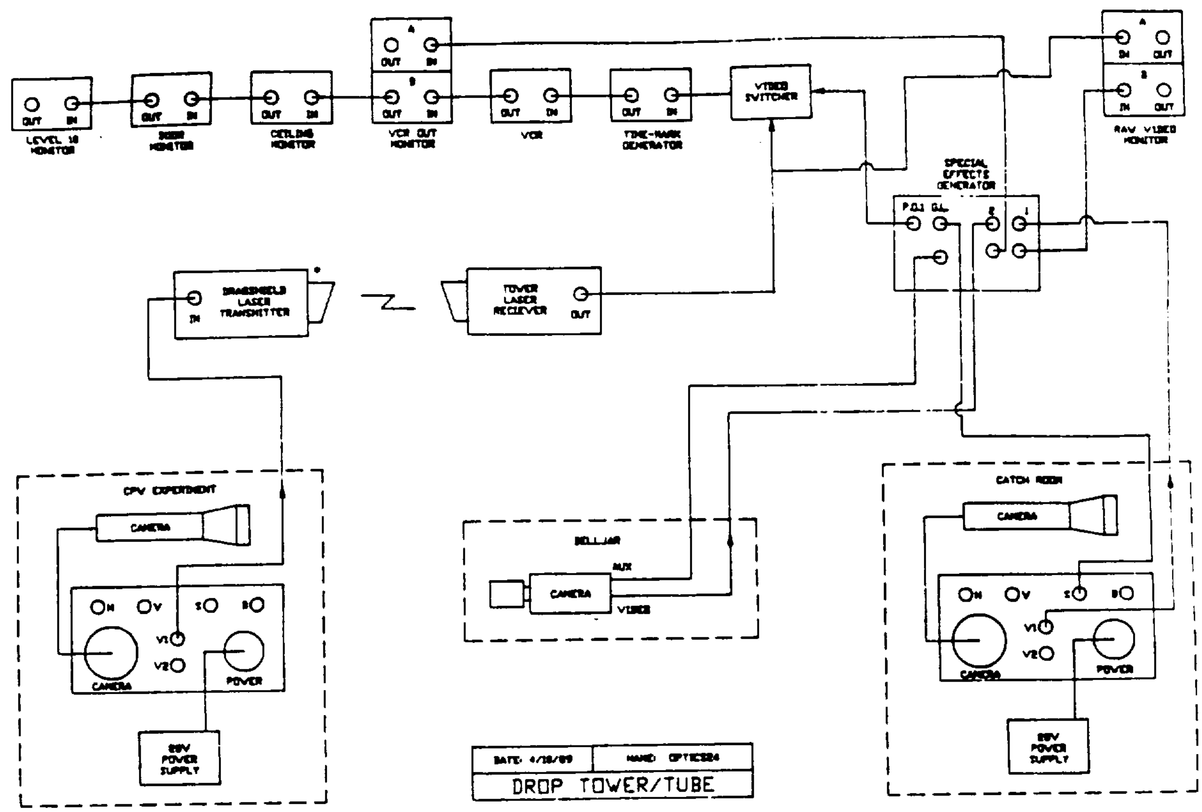

FIGURE 7.

C P W DROP TOWER EXPERIMENT
INTERFACIAL CURVATURE

BOND NUMBER DEFINITION

$$B_o = \frac{\delta g \left(d^2 / 2 \right)^2}{\sigma}$$

FIGURE 6.

PERFLUOROMETHYLCYCLOHEXANE AND ISOPROPANOL
34 deg C

1 g BEFORE RELEASE	0.0003 g 2.3 SECONDS FROM RELEASE

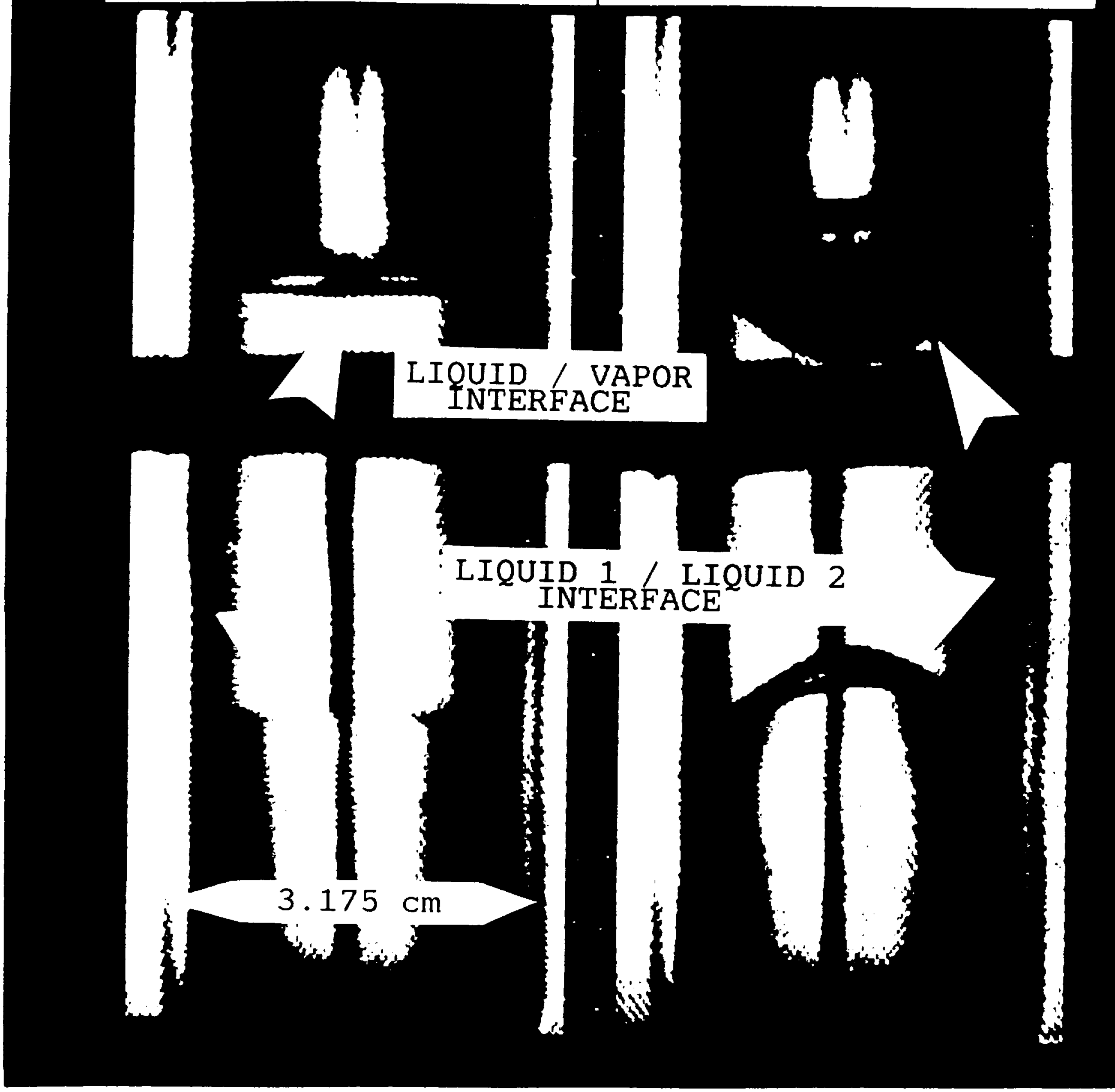

CALCULATED INTERFACE PROFILE FOR VARIOUS BOND NUMBERS. A REPRESENTS THE SUCCINONITRLE AND WATER INTERFACE; B REPRESENTS THE CYCLOHEXANE-METHANOL INTERFACE; C REPRESENTS THE INTERFACE BETWEEN DIETHYLENE GLYCOL AND ETHYL SALICYLATE; ALL AT ROOM TEMPERATURE. D IS FOR COMPARISON

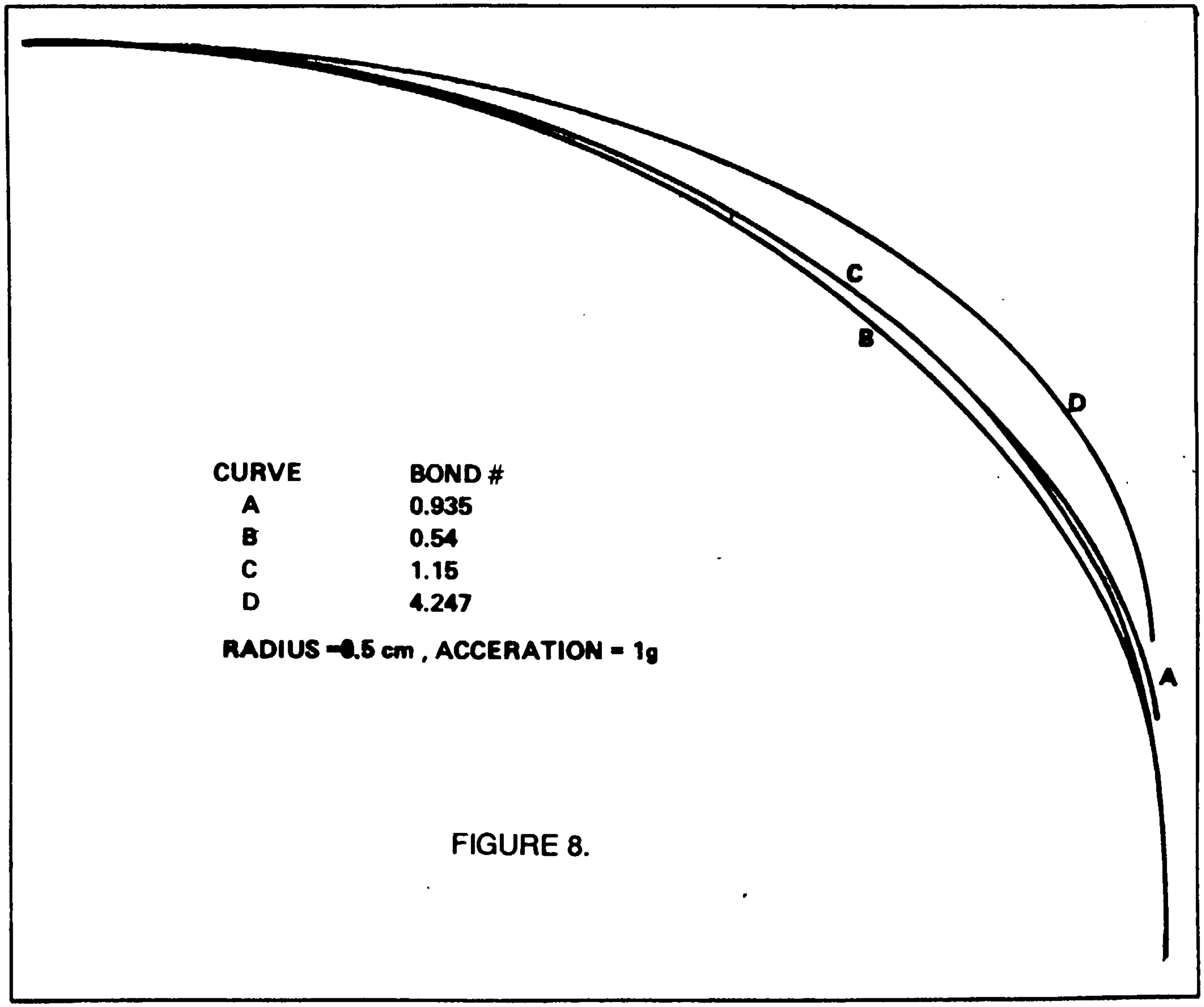

FIGURE 8.

FIGURE 10.

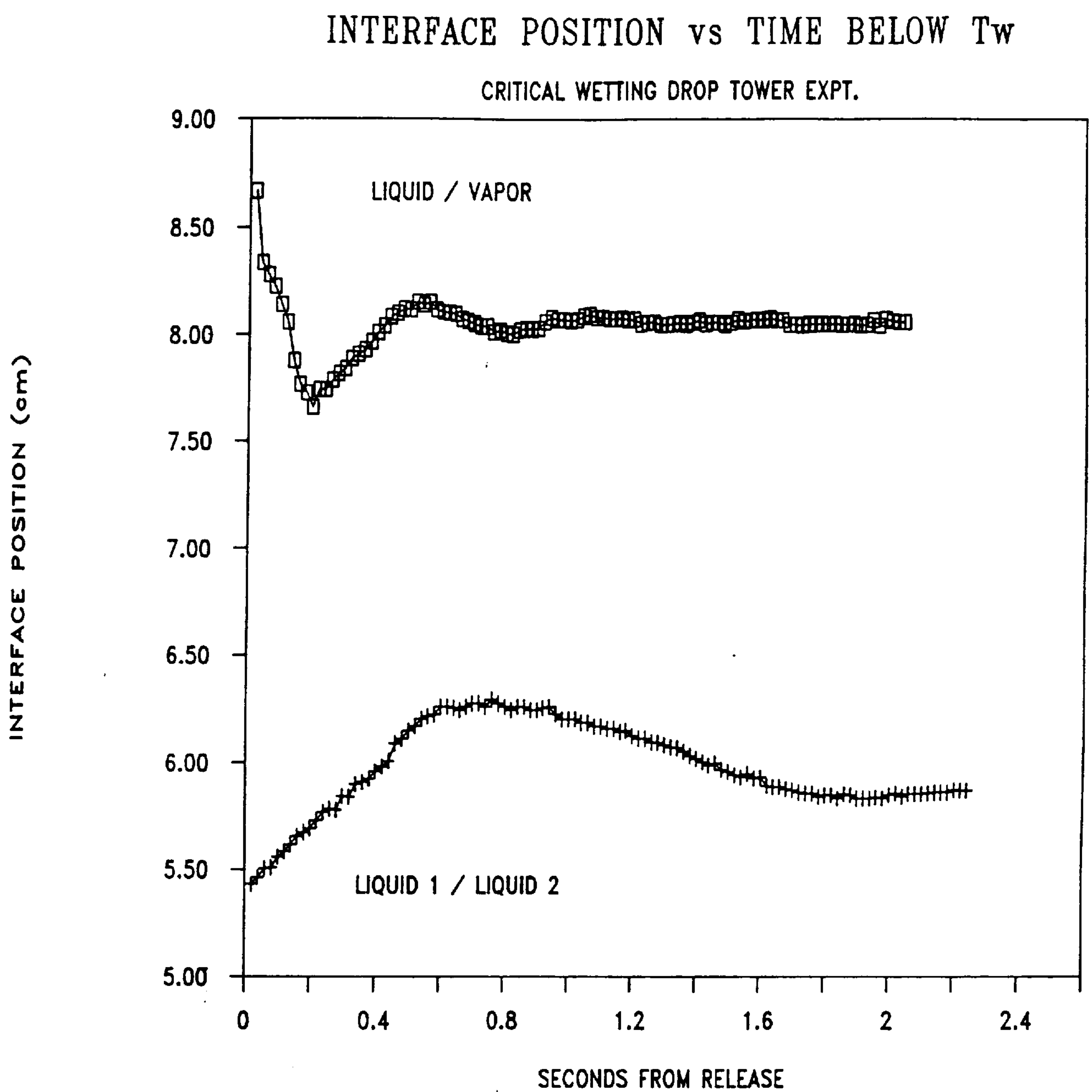
INTERFACE POSITION vs TIME BELOW Tw
CRITICAL WETTING DROP TOWER EXPT.
9.00
8.50
8.00
7.50
7.00
6.50
6.00
5.50
5.00
INTERFACE POSITION (cm)
LIQUID / VAPOR
LIQUID 1 / LIQUID 2
0
0.4
0.8
1.2
1.6
2
2.4
SECONDS FROM RELEASE

FIGURE 11.

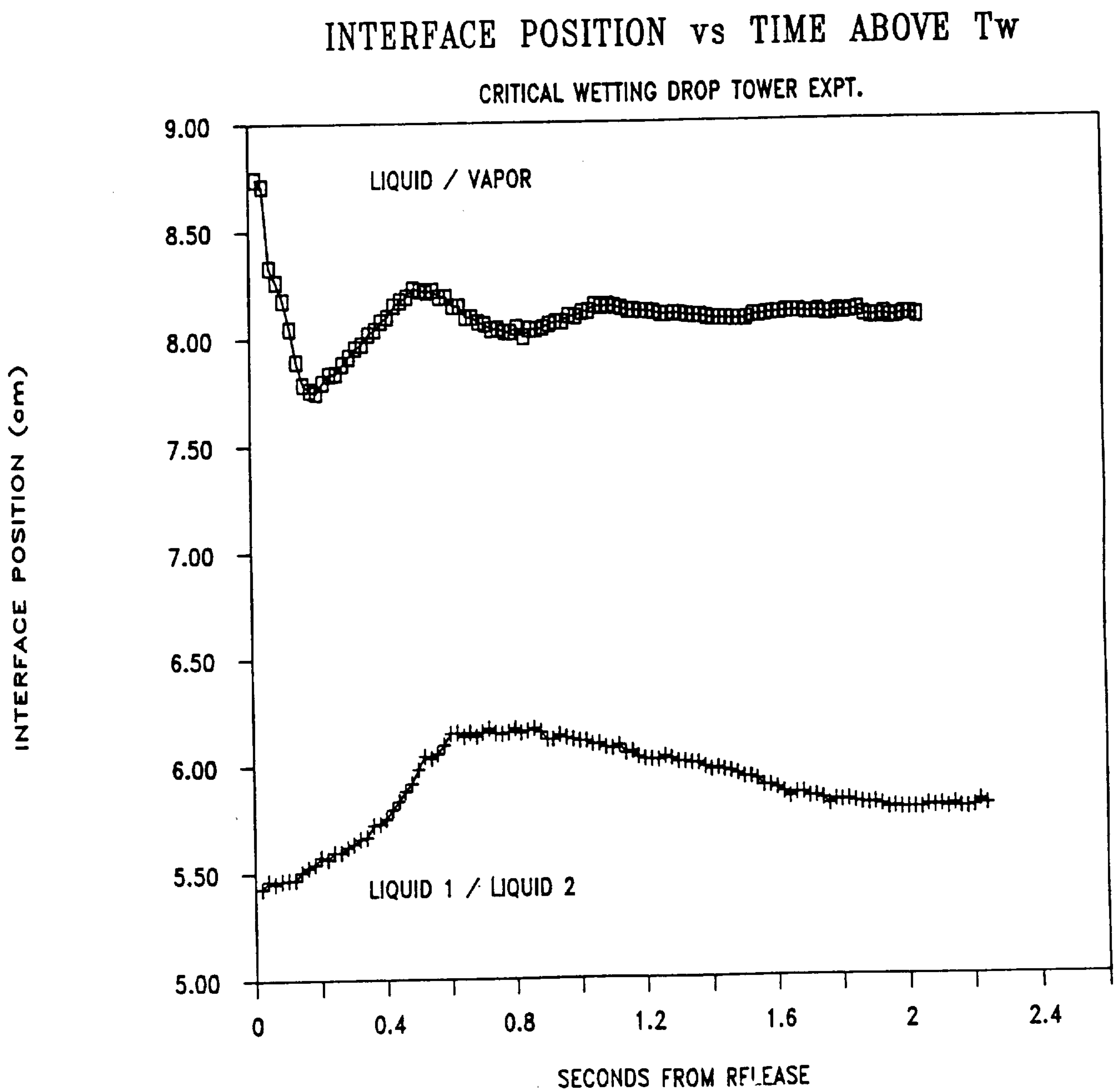
INTERFACE POSITION vs TIME ABOVE Tw
CRITICAL WETTING DROP TOWER EXPT.
LIQUID / VAPOR
LIQUID 1 / LIQUID 2
INTERFACE POSITION (cm)
SECONDS FROM RELEASE
9.00
8.50
8.00
7.50
7.00
6.50
6.00
5.50
5.00
0
0.4
0.8
1.2
1.6
2
2.4

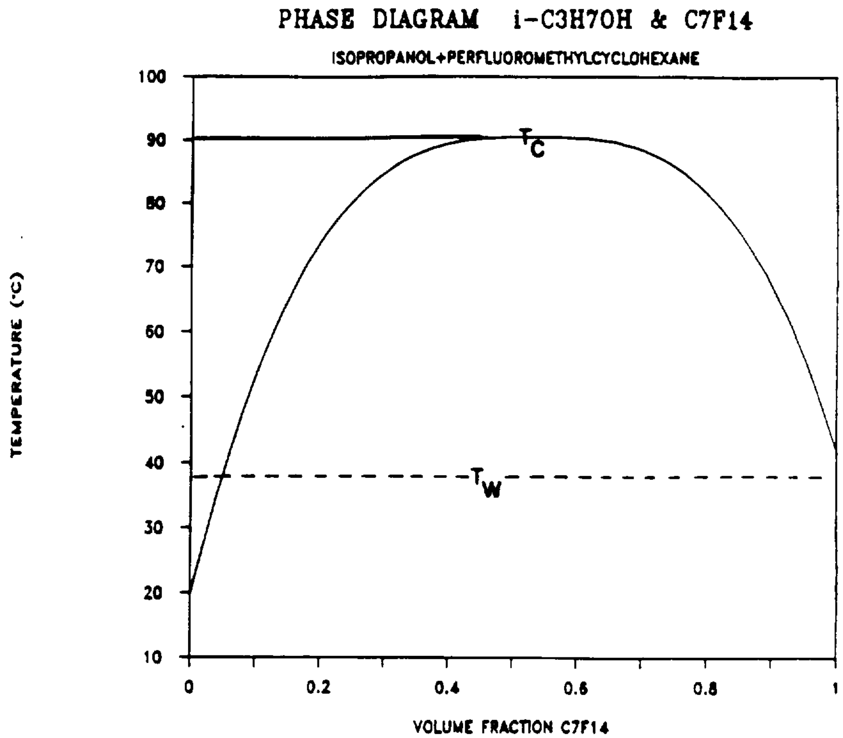

FIGURE 9.

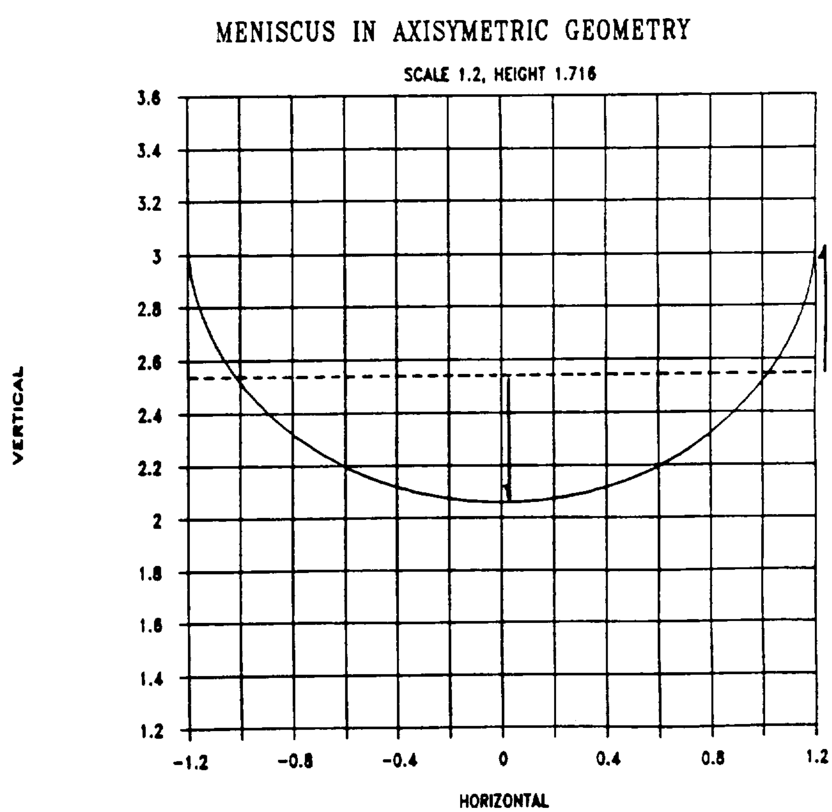

FIGURE 12.